EVALUATION OF REFLECTED FIELDS AT CAUSTIC REGIONS USING A SET OF G.O. EQUIVALENT LINE CURRENTS

John L. Volakis* and Leon Peters, Jr.
The Ohio State University
Electroscience Laboratory
Columbus, Ohio 43212

ABSTRACT

A set of equivalent electric and magnetic line currents are derived which supplement the G.O. solution in the far zone whenever one of the surface principal radii becomes very large. These hypothetical currents lie along the specular line of the surface and are shown to produce the same result as the stationary phase contribution of the physical optics integral. An example of a systematic application of such equivalent currents for the computation of the scattered field from a complex structure is also demonstrated.

This work was supported in part by the Joint Services Electronics Program under Contract N00014-78-C0049 and The Ohio State University Research Foundation

* Currently with The University of Michigan Radiation Laboratory, Department of Electrical Engineering and Computer Science, Ann Arbor, MI 48109.

I. INTRODUCTION

It is well known that the Geometical Optics (GO) field due to scattering from a surface is given in the far zone by [1,2]

$$E^{GO} = E^{i}(Q_R)\, R\sqrt{\rho_1^r \rho_2^r}\, \frac{e^{-jks}}{s} \tag{1}$$

where $E^i(Q_R)$ is the incident electric field at Q_R, R is the surface reflection coefficient, s is the far field distance from the point of reflection Q_R (see Fig. 1) to the receiver and $\rho_{1,2}^r$ are the principal radii of the reflected wavefront. In case of principal plane incidence we have

$$\rho_1^r = \frac{R_1\, \rho_1^i \cos\theta_i}{R_2 \cos\theta_i + 2\rho_1^i} \tag{2a}$$

and

$$\rho_2^r = \frac{R_2\, \rho_2^i}{R_2 + 2\rho_2^i \cos\theta_i} \tag{2b}$$

where $R_{1,2}$ are the principal radii of the surface at Q_R, $\rho_{1,2}^i$ are the principal radii of the incident wavefront and $\cos\theta_i = \hat{n} \cdot \hat{s} = -\hat{n} \cdot \hat{s}^i$ as shown in Fig. 1. It is clear that either $\rho_{1,2}^r$ can become infinite and equation (1) is then invalid. An example is that of plane wave scattering by a finite cylinder in which case

the GO term becomes indeterminate. One must then resort to a Physical Optics (PO) solution which involves the integration of the surface currents $\bar{J}_{PO} = 2\hat{n} \times \bar{H}^i$ over the lit region of the surface.

In this paper a set of equivalent line currents is introduced similar to the equivalent edge currents developed by Ryan and Peters [3] for treating caustics associated with diffracted fields. These currents reduce the solution to a line integral and will be referred to as GO equivalent line currents since they produce the same result as the GO expression of equation (1) and which remains valid when equation (1) fails. Such a solution would be inherently more accurate than is PO in that the error caused by the termination of the integration in PO (at the shadow boundary) is eliminated. Further, the GO equivalent line current can be readily improved by introducing higher order terms such as is done in the Luneberg-Kline expansion [2]. The use of the GO equivalent line current is intended to give a systematic approach for computing high frequency scattering from complex structures using the GO solution along with the Geometrical Theory of Diffraction [1]. Section III presents an application of these currents to a relatively complex structure.

II. FORMULATION OF THE GO EQUIVALENT LINE CURRENTS

Consider the incidence of a plane wave over an infinite conductive cylinder as illustrated in Fig. 2(a). The reflected field is in the $\hat{s}$ direction and is simply given by

$$E^R_{\substack{\parallel \\ \perp}} = E^i_{\substack{\parallel \\ \perp}} (\pm 1) \sqrt{\frac{r}{\rho_1}} \frac{e^{-jks}}{\sqrt{s}} \tag{3}$$

where R of equation (1) has been replaced by ± 1, $E^i_{\parallel \atop \perp}$ is polarized along $\hat{e}^i_{\parallel}$ or $\hat{e}^i_{\perp}$ and $E^R_{\parallel \atop \perp}$ is polarized along $\hat{e}^r_{\parallel}$ or $\hat{e}^r_{\perp} = \hat{e}^i_{\perp}$, respectively. Note that in Fig. 2(a), $\hat{e}^i_{\perp} = \hat{z}$ and $\hat{e}^i_{\parallel} = -\hat{\phi}^i$.

Our objective is to evaluate a set of equivalent electric (I^e) and magnetic (I^m) currents along the specular line of the cylinder, so the field produced by these currents is equal to that in equation (3). The field due to these hypothetical currents on the infinite cylinder is given by

$$E_{\parallel} = \frac{jkz_o}{4\pi} I^e \sqrt{\frac{2\pi}{k}}\, e^{-j\pi/4}\, \frac{e^{-jks}}{\sqrt{s}} \tag{4a}$$

and

$$E_{\perp} = \frac{jk}{4\pi} I^m \sqrt{\frac{2\pi}{k}}\, e^{-j\pi/4}\, \frac{e^{-jks}}{\sqrt{s}} \tag{4b}$$

where z_o is the free space impedance and k is the wave number. Equating equations (4) with the appropriate equations (3) one obtains the expressions

$$I^e_m = \begin{cases} E^i_{\parallel}\, \dfrac{\sqrt{\rho r_1}}{z_o} \sqrt{\dfrac{8\pi}{k}}\, e^{-j\pi/4} \\ -E^i_{\perp} \sqrt{\rho^r_1} \sqrt{\dfrac{8\pi}{k}}\, e^{-j\pi/4} \end{cases} \tag{5}$$

The scattered far field in the xy plane from a finite cylinder of length, ℓ, is now obtained by integrating the GO equivalent line currents in equation (5) as follows:

$$E_{\substack{\parallel \\ \perp}} = \begin{Bmatrix} -z_o \\ 1 \end{Bmatrix} \frac{e^{-jks}}{s} \frac{jk}{4\pi} \int_o^{\ell} I^e_{\substack{\parallel \\ \perp}} \, d\ell \tag{6}$$

which gives

$$E_{\substack{\parallel \\ \perp}} = -E^i_{\substack{\parallel \\ \perp}} e^{j\pi/4} \ell \sqrt{\frac{kR_1 \cos \phi^i}{4\pi}} \frac{e^{-jks}}{s} \tag{7}$$

where $\rho_1^r = R_1 \cos \phi^i/2$ has been substituted according to equation (2a). Also note that the backscattered field is obtained with $\phi^i = 0$. In Fig. 2(a) this corresponds to $\hat{s} = -\hat{s}^i = -\hat{x}$.

According to the physical optics formulation, the backscattered field will be given by

$$E^{bsc}_{\substack{\parallel \\ \perp}} = -2E^i_{\substack{\parallel \\ \perp}} \frac{e^{-jks}}{s} \frac{jk}{4\pi} \int_o^{\ell} \int_{\text{lit region}} e^{-2jkR_1(1-\cos\phi)} \cdot \cos\phi \, R_1 \, d\phi \, d\ell \tag{8a}$$

where

$$J_{PO} = \frac{2E^i}{z_o} \cos\phi \, e^{-jkR_1(1-\cos\phi)} \, . \tag{8b}$$

Employing a stationary phase approximation of the above expression and neglecting the erroneous contribution from the integral endpoints at $\phi = \pm\pi$, one obtains the result of equation (7).

The equivalent current expressions can be generalized to include oblique incidences as can the PO solution as shown in Fig. 3.

In this figure the unit vectors $\hat{t}_{I1}$ and $\hat{t}_{I2}$ correspond to the principal directions of the surface and $\hat{\tau}_{I2}$ is normal to the plane of the incidence. These are required for the computation of the principal radii associated with the reflected wavefront. The GO equivalent line currents now take the form

$$I^e = \hat{p} \frac{\hat{p} \cdot \bar{E}^i}{z_o \sin \beta_o^i} \sqrt{\rho_\tau^r} \sqrt{\frac{8\pi}{k}} e^{-j\pi/4} \tag{9a}$$

and

$$I^m = -\hat{p} \frac{(\hat{p} \times \hat{s}^i) \cdot \bar{E}^i}{\sin \beta_o^i} \sqrt{\rho_\tau^r} \sqrt{\frac{8\pi}{k}} e^{-j\pi/4} \tag{9b}$$

where $\hat{p}$ is the unit vector tangent to the specular line and as usual

$$\beta_o^i = \cos^{-1} (-\hat{s}^i \cdot \hat{p}) \quad . \tag{10}$$

For a plane wave incidence and infinite R_2, ρ_τ^r is equal to ρ_1^r (the only finite radius) provided the line of integration is along the surface direction associated with R_2. However if the convex reflection surface is doubly curved, then the line of integration should follow the path tangent to the principal surface direction corresponding to the largest radius of curvature (R_2). Such a path choice ensures that the GO line integral in (6) will reduce to the usual GO field expression when evaluated via the stationary phase. Further, ρ_τ^r may be chosen as the principal radius associated with the direction closest to $\hat{t}_{I2}$. This should be adequate for engineering purposes and can be applied also to the case of arbitrary incidences,

provided $R_2 >> R_1$ which is a condition imposed earlier. If R_2 is not very large then clearly the use of the equivalent current integration is not required.

The total reflected field from the smooth surface is the sum of the fields caused by the GO equivalent line currents I^e and I^m, i.e.

$$\bar{E} = \bar{E}^e + \bar{E}^m \quad , \tag{11}$$

where $\bar{E}^e$ and $\bar{E}^m$ are associated with I^e and I^m, respectively.

The limitation and accuracy of the above procedure is, of course, comparable to that of the traditional GO expression. In general, the surface radii of curvature must be greater than $\lambda/4$, where λ denotes the wavelength. For smaller radii a more accurate reflection coefficient must be used in the GO expression of equation (1). In addition, if the observation point is not at the specular direction then the result of this analysis will only be valid in the main lobe region. Outside this region the scattered field must be evaluated by considering the edge diffraction effects from the surface terminations which correspond to the endpoints of the integral in (6).

III. APPLICATION TO COMPLEX GEOMETRIES

The GO equivalent current concept was systematically applied for the evaluation of the backscattered field caused by the structure of Fig. 4 in the xz plane (nose region). This structure consists of a toroidal lip over an ogive. The usual GO analysis which includes the reflection from the lip (see Fig. 5), the double and triple reflection between the ogive and the lip as well as the GO fields of

the ogive (see Appendix), gives correct results in part of the region only. The results are shown in Fig. 6. As seen, the GO solution fails for incidences near the x-axis due to the congruence of the singly reflected rays from the lip and also whenever the multiply reflected fields cause a similar caustic effect.

In this case, the doubly reflected field has a caustic at $\theta \simeq 65$ degrees where the transverse (to the plane of incidence) radius of curvature of the reflected wavefront from the lip becomes infinite. An analytical evaluation of this caustic location is rather involved but can be found in [4]. In the caustic region, the GO equivalent currents can be applied to obtain a bounded solution which is comparable to the physical optics results. However, since one of the principal radius of the toroid remains large, the GO equivalent current integration may be also extended outside the caustic region. This was indeed done for the present geometry.

Additional backscatter mechanisms in the xz plane of the structure are also caused by the curved edge formed at the junction of the cylindrical lip with the ogival surface. However, this does not need to be considered separately since the endpoints contribution of the GO equivalent current line integral corresponds approximately to the scattering of this mechanism for the given principal plane patterns. Further, the hollow pipe with the cylindrical lip over the ogive is of infinite extent and therefore no contribution from its internal portion is considered here. As the incidence angle θ increases, part of the rim becomes shadowed and can only be illuminated with surface diffracted

rays from the surface of the ogive. The current along this portion of the rim specular line was found via an extrapolation routine similar to that discussed in [5].

The Radar Cross Section (RCS) patterns obtained in the xz plane using the GO equivalent current formulation are now shown in Fig. 7. The singly reflected field was obtained by integrating along the rim line given by

$$\bar{P}_{r_1} = \hat{x}\,\rho_I \sin\theta + \hat{y}(h + a + \rho_I \cos\theta)\sin\theta_I + \hat{z}(h + a + \rho_I \cos\theta)\cos\theta_I \qquad (12)$$

which is the specular line on the lip producing the field caustic. The parameters, ρ_I, h and a are defined in Fig. 4. The angle θ_I is measured from the z-axis and in the yz plane as shown in Fig. 3. The doubly reflected field was obtained by integrating over the rim line given by

$$\bar{P}_{r_2} = \hat{x}\,\rho_I \cos\beta_{r_2} + \hat{y}(h + a - \rho_I \sin\beta_{r_2})\sin\theta_I + \hat{z}(h + a - \rho_I \sin\beta_{r_2})\cos\theta_I \quad . \qquad (13)$$

The parameter β_{r_2} in the above expression is shown in Fig. 5 and satisfies the backscatter condition

$$\theta_i^{r^2} + \theta_{iI}^{r^2} = \pi/2 \quad . \tag{14}$$

Note that (12) and (13) define circular lines over the toroidal lip and pass through the associated specular point in the xz plane. Such a definition is according to our postulation in the previous section.

For the present application there was no need to employ the GO equivalent current concept for the triply reflected field because of the non-existence of a caustic and its relatively smaller contribution as shown in Fig. 6. The total backscattered field was computed by summing the individual components as follows:

$$\bar{E}^{bsc} = \bar{E}_{GO}^{R} + \bar{E}_{1}^{R} + 2\bar{E}_{2}^{RR} + \bar{E}_{3}^{RRR} \quad , \tag{15}$$

where $\bar{E}_{GO}^{R}$ = GO field from the surface of the ogive,

$\bar{E}_{1}^{R}$ = singly reflected field from lip,

$\bar{E}_{2}^{RR}$ = doubly reflected field between the ogive and lip and

$\bar{E}_{3}^{RRR}$ = triply reflected field between the ogive and the lip.

The evaluation of the GO equivalent line currents for the doubly reflected field required the knowledge of the field first reflected from the surface of the ogive. The determination of this component involved the tracing of the reflected rays from the ogive to each specular rim point given in equation (13). This ray tracing routine is outlined in [5] and a detailed description of the parameters used for the evaluation of the equivalent line currents can be found in [4].

The reader will further note that the singly and doubly reflected field curves computed via the GO equivalent line currents in Fig. 7, differ to some degree from those in Fig. 6 even outside the caustic region. As mentioned above this is due to the inclusion of the diffraction from the junction of the lip with the ogive when the equivalent current integration was employed. Beyond $\theta \approx 122$ degrees, the whole lip is shadowed. In this region, the given backscatter patterns in Figs. 6 and 7 include the contribution of the surface diffracted ray [6] from the ogive and through the stationary point on the lip. It is important to note that continuity of the total field is still maintained at this transition point.

IV. CONCLUSION

A set of equivalent electric and magnetic line currents were developed which can be used to supplement the usual GO expression. The field produced by these currents remains bounded when one of the radii of the reflected wavefront becomes very large in which case the GO solution fails. It was shown that the GO equivalent current line integral produces the same result as the stationary phase contribution of the physical optics surface integral. A general application of these currents was demonstrated and compared to the usual GO solution.

This equivalent current solution produces more accurate results than the PO solution for a general type of scatterer since it eliminates the shadow boundary discontinuity of PO. In addition, it introduces none of the tedious computations that would appear in PO if the radius of curvature became angular (ϕ) dependent.

APPENDIX

The expressions used for evaluating the GO field of the ogive in the xy plane are given by [7]

$$\bar{E}_{GO}(\theta) = -\bar{E}^i(0)\frac{e^{-jks}}{s}\begin{cases}\dfrac{\sqrt{R_1 R_2^{GO}}}{2} e^{-j2k\bar{S}_{GO}\cdot\hat{s}^i} & \text{for } 0 < \theta < \alpha \\ \dfrac{R_1 \sin\alpha}{4\pi} e^{-j2k\bar{S}_{tip}\cdot\hat{s}^i} & \text{for } \theta = \alpha \\ \dfrac{j\lambda \tan^2\alpha\, e^{-j2k\bar{S}_{tip}\cdot\hat{s}^i}}{8\pi \sin^3\theta[1-\tan^2\alpha\cot^2\theta]^{3/2}} & \text{for } \alpha < \theta \leq \pi/2\end{cases} .$$

The result in the region of $\alpha < \theta < \pi/2$ is still singular when θ is close to α. Therefore, for practical purposes the value of $E_{GO}(\theta = \alpha)$ was used until $E_{GO}(\theta) \leq E_{GO}(\theta = \alpha)$. The effect of this is evident in the patterns of Figs. 6 and 7. The definition of the various parameters in the above equation are (see Fig. 4):

$$\bar{S}_{GO} = R_1[\hat{x}\sin\theta + \hat{z}(\cos\theta - \cos\alpha)] ,$$

$$\bar{S}_{tip} = \hat{x}R_1 \sin\alpha$$

and

$$R_2^{GO} = R_1\left(1 - \frac{\cos\alpha}{\cos\theta}\right) .$$

$\bar{S}_{GO}$ is the position vector corresponding to the ogive's specular point, $\bar{S}_{tip}$ is the vector defining the ogive tip and $\bar{R}_2^{GO}$ is the transverse principal radius of the ogive's surface at the point S_{GO}.

REFERENCES

1. R. G. Kouyoumjian and P. H. Pathak, "A Uniform Geometrical Theory of Diffraction for an Edge in a Perfectly Conducting Surface," Proc. of the IEEE, Vol. 62, pp. 1448-1461, 1974.
2. M. Kline, "An Asymptotic Solution of Maxwell's Equations," Commun. Pure and Appl. Math., Vol. 4, pp. 225-262, 1951.
3. C. E. Ryan and L. Peters, Jr., "Evaluation of Edge-Diffracted Fields Including Equivalent Currents for Caustic Regions," IEEE Trans. on Antennas and Propagat., Vol. AP-17, pp. 292-299, 1969; see also correction to this paper in Vol. AP-18, p. 275, 1970.
4. J. L. Volakis, "Electromagnetic Scattering from Inelts and Plates Mounted on Arbitrary Smooth Surfaces," Chapter V, Ph. D. Dissertation, The Ohio State Univ., Dept. of Electrical Engineering, 1982.
5. J. L. Volakis, W. D. Burnside and L. Peters, Jr., "Electromagnetic Scattering from Appendages on a Smooth Surface," IEEE Trans. on Antennas and Propagat., Vol. AP-33, July 1985.
6. P. H. Pathak, W. D. Burnside and R. J. Marhefka, "A Uniform GTD Analysis of the Diffraction of Electromagnetic Waves by a Smooth Convex Surface," IEEE Trans. on Antennas and Propagat., Vol. AP-28, pp. 631-642, 1980.
7. L. Peters, Jr., "Memorandum on the Echo Area of Ogives," Electroscience Lab., Report 601-7, The Ohio State Univ., Jan. 1956.

LIST OF FIGURES

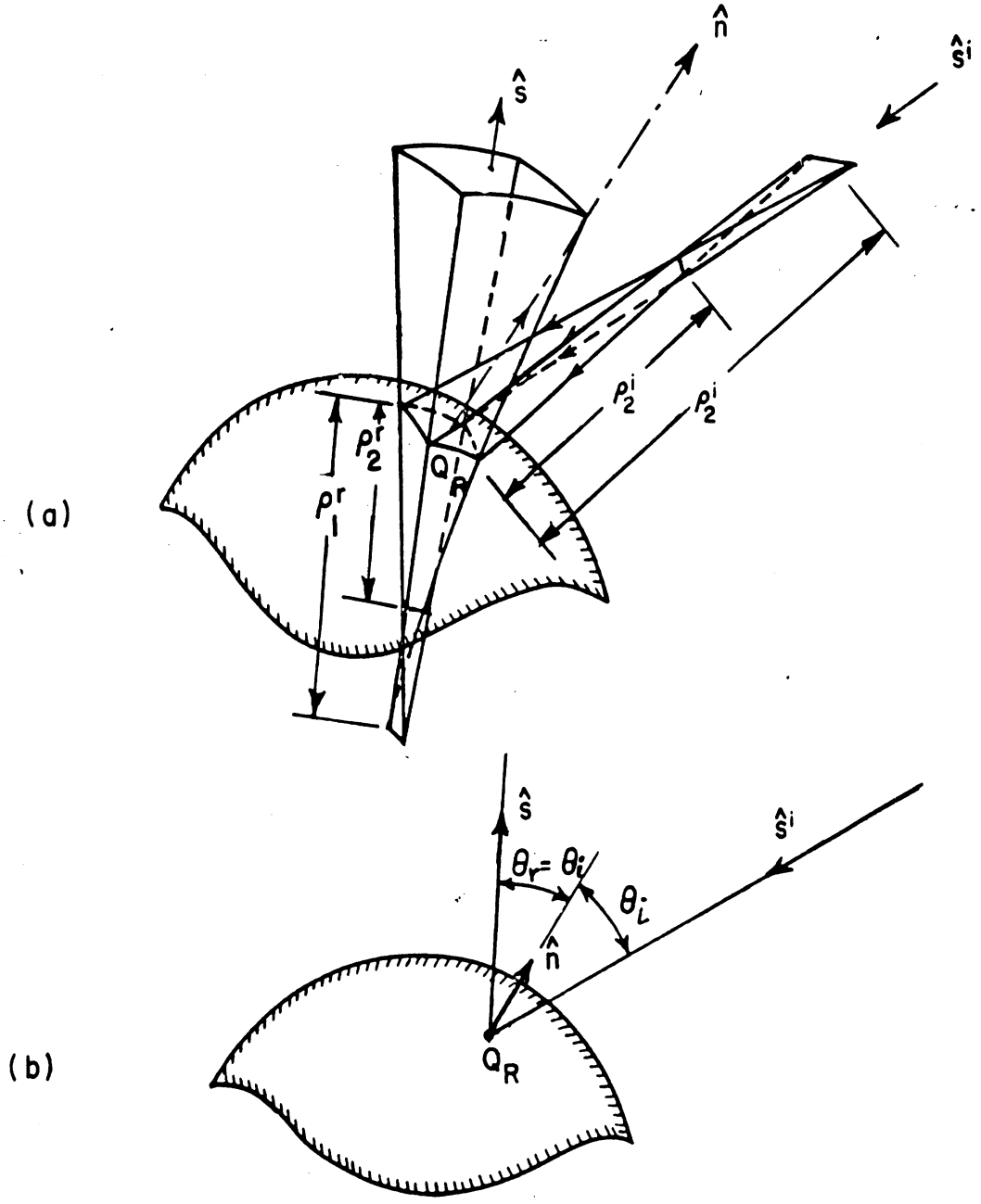
(a)
$\hat{n}$
$\hat{s}^i$
$\hat{s}$
ρ_2^i
ρ_2^i
ρ_2^r
Q_R
ρ_1^r
(b)
$\hat{s}$
$\hat{s}^i$
$\theta_r = \theta_i$
θ_i
$\hat{n}$
Q_R

Figure 1

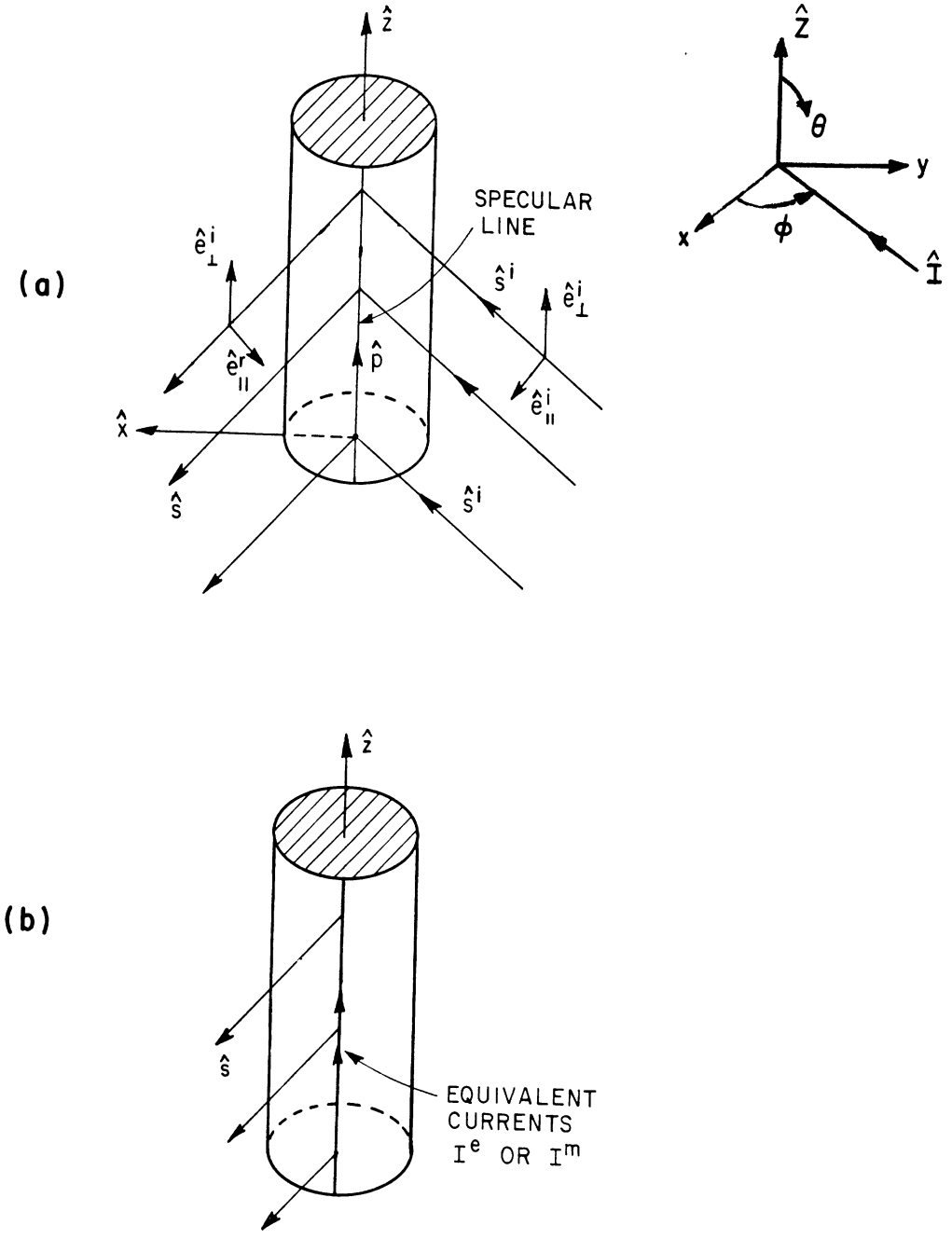
(a)
$\hat{z}$
SPECULAR LINE
$\hat{e}^i_\perp$
$\hat{s}^i$
$\hat{e}^i_\perp$
$\hat{e}^r_\parallel$
$\hat{p}$
$\hat{e}^i_\parallel$
$\hat{x}$
$\hat{s}$
$\hat{s}^i$
$\hat{Z}$
θ
y
x
ϕ
$\hat{I}$
(b)
$\hat{z}$
$\hat{s}$
EQUIVALENT CURRENTS
I^e OR I^m

Figure 2.

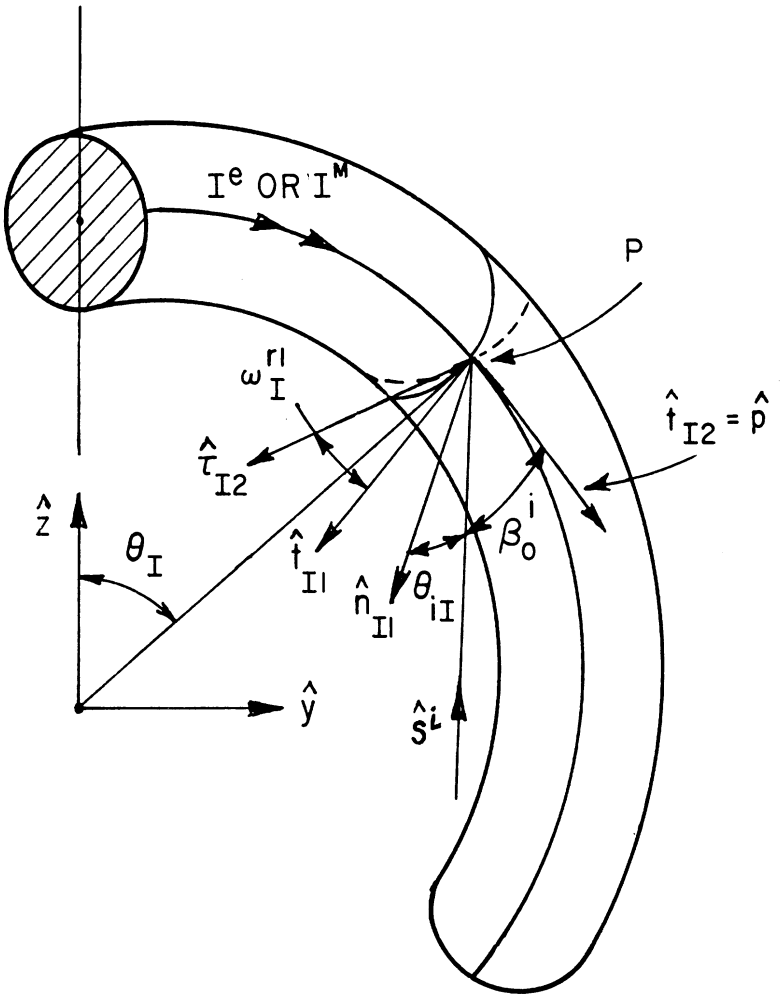
I^e OR I^M
P
ω_I^{rI}
$\hat{t}_{I2} = \hat{p}$
$\hat{\tau}_{I2}$
$\hat{z}$
θ_I
$\hat{t}_{I1}$
β_o^i
$\hat{n}_{I1}$
θ_{iI}
$\hat{y}$
$\hat{s}^i$

Figure 2

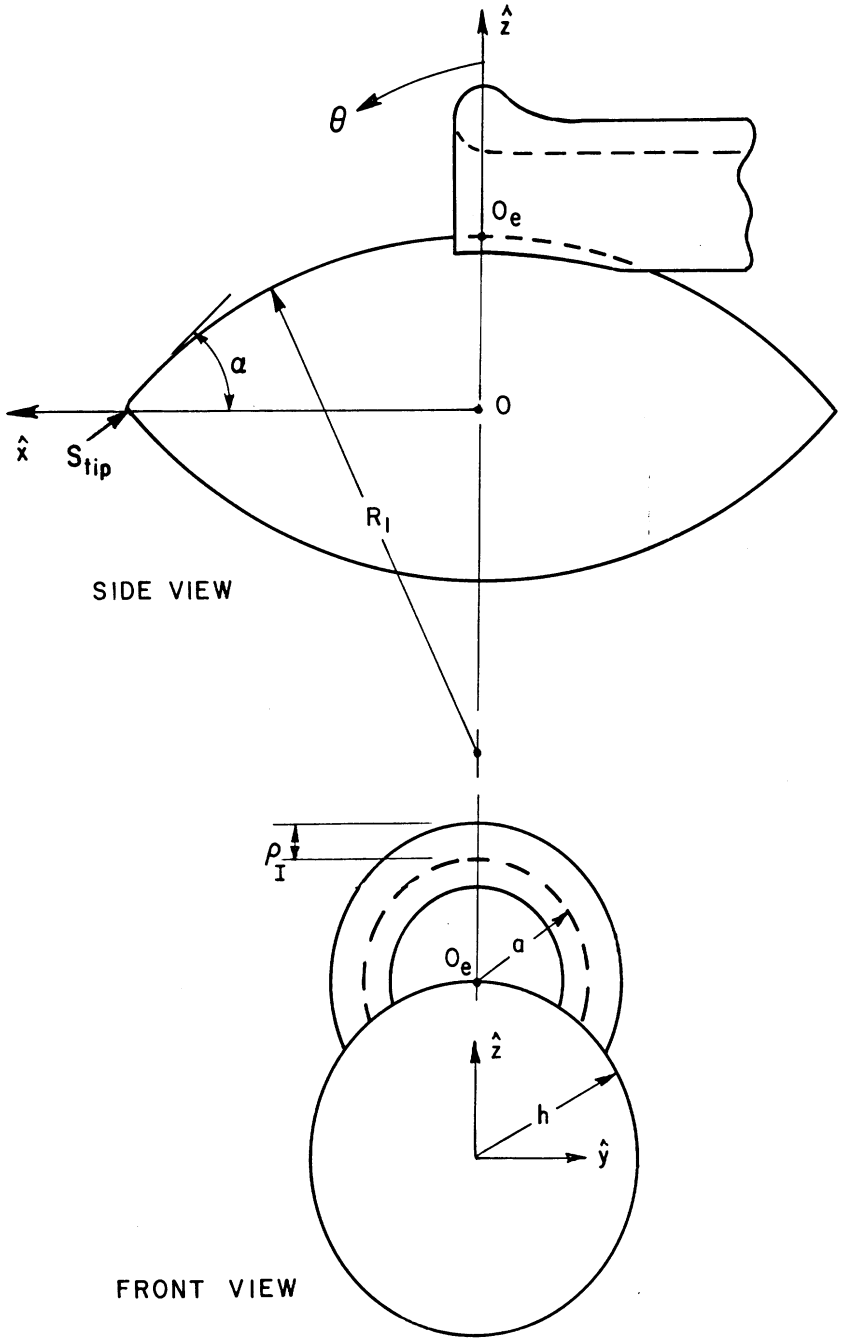
$\hat{z}$
θ
O_e
α
O
$\hat{x}$
S_{tip}
R_I
SIDE VIEW
ρ_I
O_e
a
$\hat{z}$
h
$\hat{y}$
FRONT VIEW

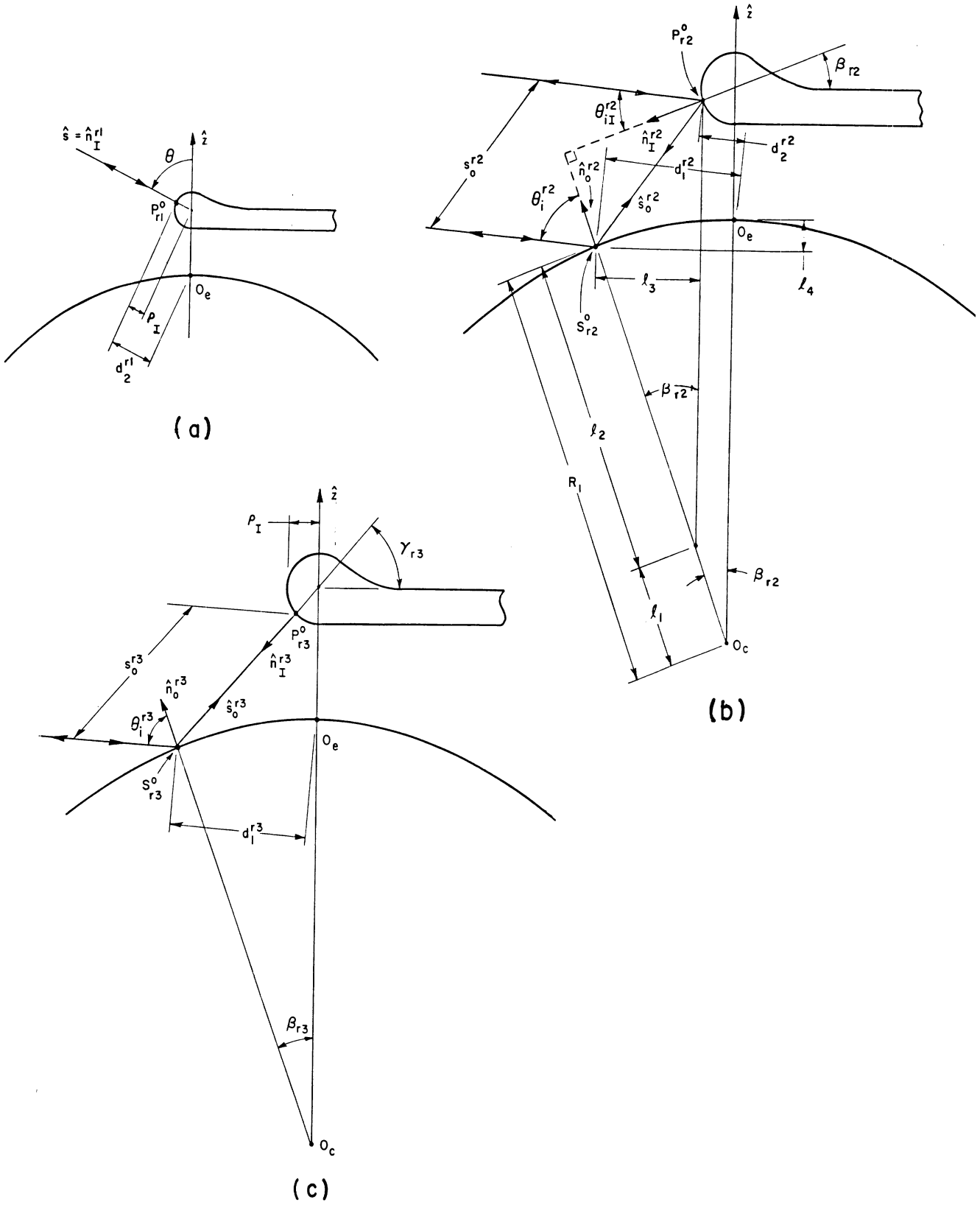
(a)
(b)
(c)

(a)

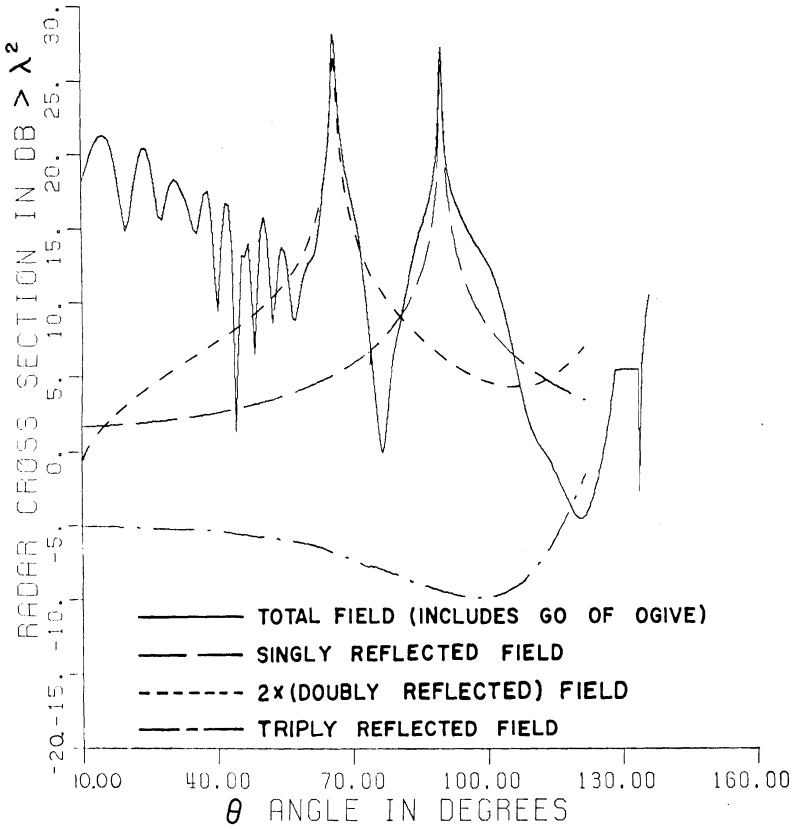
RADAR CROSS SECTION IN DB > λ²
30.
25.
20.
15.
10.
5.
0.
-5.
-10.
-15.
-20.
TOTAL FIELD (INCLUDES GO OF OGIVE)
SINGLY REFLECTED FIELD
2x(DOUBLY REFLECTED) FIELD
TRIPLY REFLECTED FIELD
10.00
40.00
70.00
100.00
130.00
160.00
θ ANGLE IN DEGREES

(b)

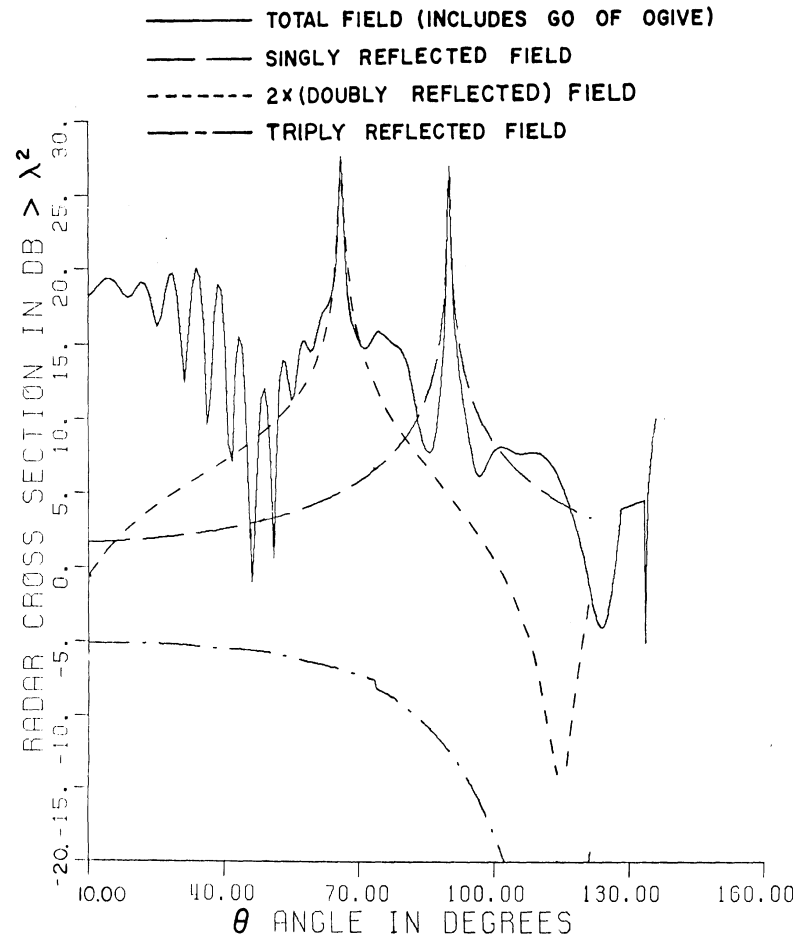
TOTAL FIELD (INCLUDES GO OF OGIVE)
SINGLY REFLECTED FIELD
2x(DOUBLY REFLECTED) FIELD
TRIPLY REFLECTED FIELD
RADAR CROSS SECTION IN DB > λ²
30.
25.
20.
15.
10.
5.
0.
-5.
-10.
-15.
-20.
10.00
40.00
70.00
100.00
130.00
160.00
θ ANGLE IN DEGREES

(a)

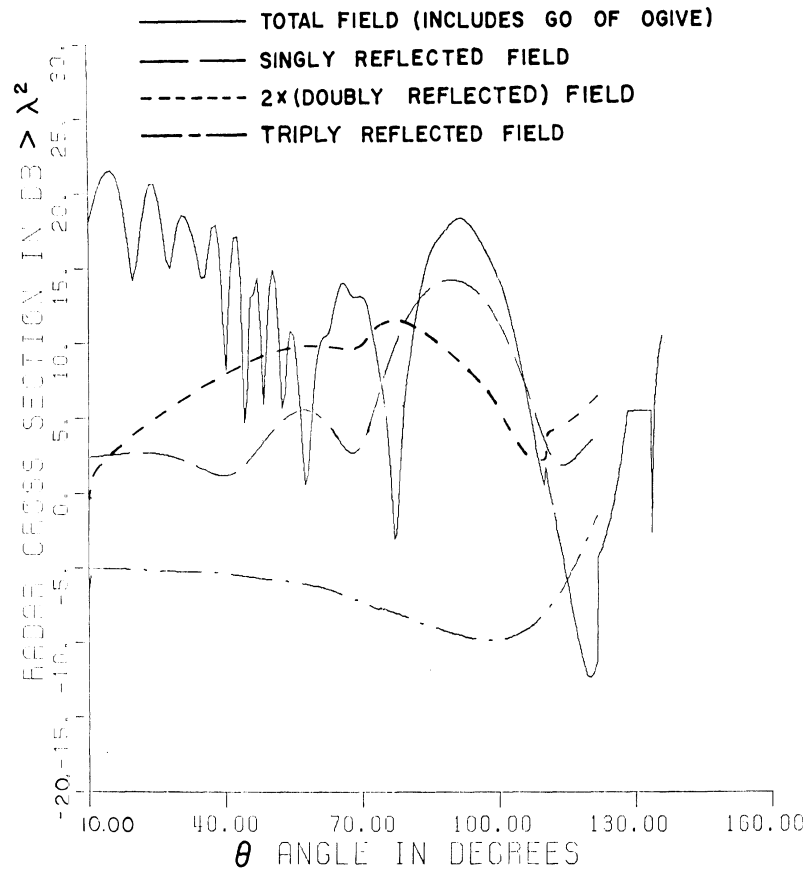
TOTAL FIELD (INCLUDES GO OF OGIVE)
SINGLY REFLECTED FIELD
2x(DOUBLY REFLECTED) FIELD
TRIPLY REFLECTED FIELD
RADAR CROSS SECTION IN DB > λ²
-20. -15. -10. -5. 0. 5. 10. 15. 20. 25. 30.
10.00 40.00 70.00 100.00 130.00 160.00
θ ANGLE IN DEGREES

(b)

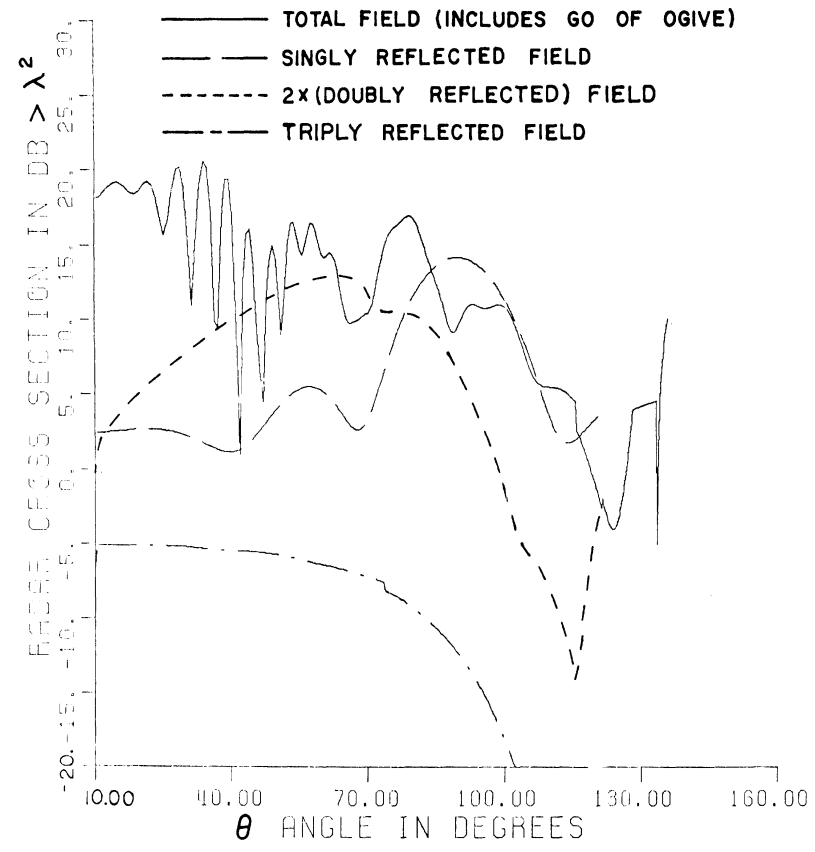
TOTAL FIELD (INCLUDES GO OF OGIVE)
SINGLY REFLECTED FIELD
2x(DOUBLY REFLECTED) FIELD
TRIPLY REFLECTED FIELD
RADAR CROSS SECTION IN DB > λ²
-20. -15. -10. -5. 0. 5. 10. 15. 20. 25. 30.
10.00 40.00 70.00 100.00 130.00 160.00
θ ANGLE IN DEGREES